

Scaling laws for pulsed electrohydrodynamic drop formation

C.-H. Chen, D. A. Saville, and I. A. Aksay^{a)}

Department of Chemical Engineering, Princeton University, Princeton, New Jersey 08544

(Received 22 August 2005; accepted 23 August 2006; published online 20 September 2006)

A pulsed electrohydrodynamic jet can produce on-demand drops much smaller than the delivery nozzle. This letter describes an experimentally validated model for electrically pulsed jets. Viscous drag in a thin nozzle limits the flow rate and leads to intrinsic pulsations of the cone jet. A scale analysis for intrinsic cone-jet pulsations is derived to establish the operating regime for drop deployment. The scaling laws are applicable to similar electrohydrodynamic processes in miniaturized electro spraying systems. © 2006 American Institute of Physics.

[DOI: 10.1063/1.2356891]

Among contemporary techniques for drop generation, pulsed electrohydrodynamic (EHD) jetting may be the only one that can produce drops on demand with dimensions a decade or so smaller than the nozzle.^{1,2} The large neck-down ratio derives from the EHD cone-jet transition produced by an external voltage pulse.³ This transition is fundamental to electro spray ionization⁴ and can be experienced by an isolated charged drop or a pendent drop subject to an external field. Although similar, there are important differences between the stability and dynamics of these two cases.^{5–8} Here, we present a scaling analysis that captures the essential physics of intrinsically pulsating cone-jet transition. Although supported by our experimental results, the underlying assumptions of the scaling discussed below are subject to further validation.

EHD cone jets pulsate in response to intrinsic processes or external stimuli.⁹ Juraschek and Rollgen reported two intrinsic pulsating modes and explained pulsations as the imbalance between the supply and loss of liquid in the entire cone volume (low frequencies) or in the cone's apex (high frequency).¹⁰ Marginean *et al.* extended this work using high-speed imaging and provided direct evidence linking Taylor cone pulsations to electro spray current oscillations.¹¹ Externally pulsed electro sprays achieve higher sensitivity and better signal-to-noise ratios compared to their steady counterparts.⁹ Externally pulsed cone jets were also exploited by Yogi *et al.*³ to generate pico- to femtoliter droplets. Despite considerable experimental efforts, quantitative models are not available to relate pulsing characteristics such as flow rate and pulsation frequency to experimental parameters. We extend the theoretical work of Fernandez de la Mora⁸ and Fernandez de la Mora and Loscertales¹² to describe intrinsically pulsating cone jets.

Our configuration for EHD drop production, as shown in Fig. 1(a) and detailed in Sec. A1 of Ref. 13, resembles the system described by Yogi *et al.* and is closely related to the configuration for miniaturized electro spraying (or nanoelectro sprays).¹⁴ Miniaturized electro spraying has gained popularity in the past decade for its low reagent consumption and high ion transmission efficiency at small flow rates.¹⁵ In miniaturized electro spraying, a micron-scale nozzle is used instead of a millimeter-scale one,¹⁴ and the

flow rate is typically self-regulated.¹⁶ The main difference between our setup and that for electro spraying is that breakup is avoided during fluid transit from the nozzle to the substrate by using a much shorter nozzle-to-collector separation. Hence, instead of a spray, a series of drops is collected as a single entity at a given location on the surface.

Figure 1(b) shows a sequence of representative images depicting the EHD drop generation process. Initially, the pressure head is adjusted such that the static liquid meniscus is almost approximately flat at the nozzle exit. When an external voltage pulse is applied, the liquid meniscus deforms into a Taylor cone,¹⁷ and a jet is emitted. The volume of a collected drop is proportional to the pulse duration minus the time delay to form a Taylor cone (≈ 3.6 ms for the present

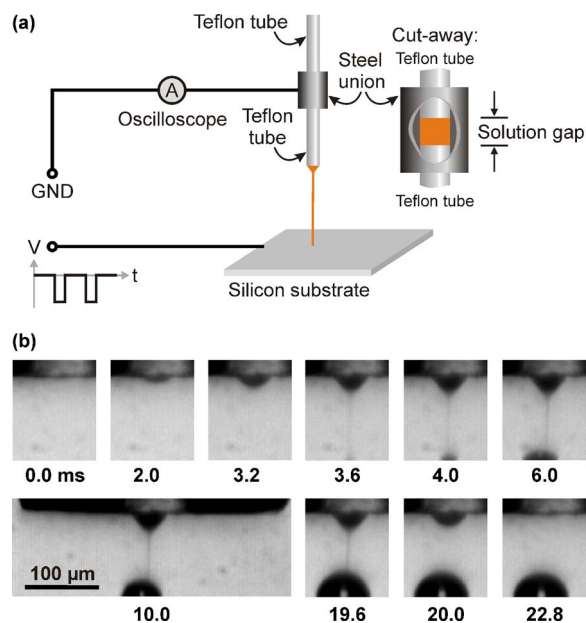


FIG. 1. (a) Schematic of the EHD drop generation system. When a voltage is applied between the Teflon nozzle (through a metal union) and the silicon substrate, the initially flat water meniscus is deformed into a Taylor cone, and a jet is emitted. A drop can be produced on the substrate using a voltage pulse, which leads to pulsed cone jets. (b) EHD drop generation process at successive times. An external voltage of 1.6 kV with a 20 ms pulse duration was applied to de-ionized water within a 50 μm inner-diameter (i.d.) Teflon nozzle. The camera was triggered on the rising edge of the pulse. The drop formation process appeared steady with a camera frame rate of 2500 frames per second (fps) and exposure time of 394 μs . The slight asymmetry was a result of skewed liquid accumulation that modifies electric field distribution close to the substrate.

^{a)} Author to whom correspondence should be addressed; electronic mail: iaksay@princeton.edu

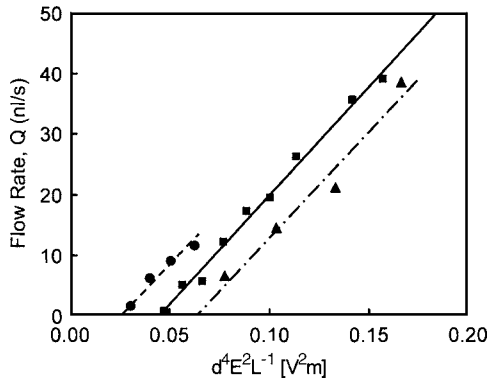


FIG. 2. Drop formation flow rate data illustrating the $Q \sim Q_c \sim d^4 E^2 L^{-1}$ scaling law. Teflon nozzles with three different combinations of inner diameters (d), lengths (L), and nozzle-to-collector separations (S) were used: (●) $d=50 \mu\text{m}$, $L=30 \text{ mm}$, $S=110 \mu\text{m}$; (■) $d=75 \mu\text{m}$, $L=41 \text{ mm}$, $S=140 \mu\text{m}$; (▲) $d=100 \mu\text{m}$, $L=41 \text{ mm}$, $S=230 \mu\text{m}$. The voltage (V) was varied between 1.2 and 2.0 kV; the nominal field strength was $\bar{E}=V/S$. The solid line is a linear regression fit to the flow rate for a 75 μm -i.d. nozzle with an R^2 constant of 0.991. The dashed lines are linear fits to the data for 50- and 100- μm -i.d. nozzles, respectively, with slopes equal to that of the solid line.

case). At the end of the 20 ms pulse, jetting stops and the conical shape gradually relaxes back to a state without electric stress (at 22.8 ms). The cone and drop formation rates extracted from Fig. 1(b) are approximately equal; this equivalence holds under a variety of conditions (Sec. A2 of Ref. 13). The empirical equivalence suggests that the flow is drag limited, i.e., the drop formation rate is not determined by the EHD process, but by the balance between electric stress at the liquid/air interface and the viscous drag in the thin nozzle. Given the large length/diameter ratio for the nozzle, and the relatively small Reynolds number, the drop deployment rate Q can be estimated as the cone formation rate Q_c , in terms of a Poiseuille-type relation,

$$Q \approx Q_c \sim \frac{\pi d_n^4}{128 \mu L} \left(\frac{\epsilon_0 E_0^2}{2} - \frac{2\gamma}{d_n} + \Delta P \right), \quad (1)$$

where μ is the viscosity of the liquid, d_n and L are the inner diameter and length of the nozzle, E_0 is the scale for external electric field, γ is the surface tension of the air/liquid interface, and ΔP is the hydrostatic pressure with respect to the nozzle exit. In Eq. (1), the electric pressure ($\epsilon_0 E_0^2/2$), capillary pressure ($2\gamma/d_n$), and hydrostatic pressure (ΔP , applied by fluid in the reservoir) drive flow through the thin nozzle. Using empirical conical volume-time data (Fig. A1 of Ref. 13), i.e., the rate at which the Taylor cone forms and retracts, Q_c and $Q_{c,r}$, Eq. (1) can be rewritten as

$$Q_c + Q_{c,r} \sim \pi d_n^4 \epsilon_0 E_0^2 / (256 \mu L). \quad (2)$$

The flow rate scaling is shown in Fig. 2 which presents drop formation rates with nozzles of three different inner diameters as a function of increasing voltage. From Eq. (1), the flow rate should scale as $Q \sim d^4 E^2 L^{-1}$, which is supported by Fig. 2 where the nominal electric field was taken as the applied voltage divided by the nozzle-to-collector separation ($\bar{E}=V/S$). The proportionality constants for all three different nozzle sizes are identical, to within experimental uncertainty. Furthermore, the empirical proportionality constant, $(Q_c + Q_{c,r}) / (d^4 V^2 S^{-2} L^{-1}) = 3.6 \times 10^{-10} \text{ m}^2 \text{ s}^{-1} \text{ V}^{-2}$, is very close to the theoretical value, $\pi \epsilon_0 / 256 \mu = 1.1 \times 10^{-10} \text{ m}^2 \text{ s}^{-1} \text{ V}^{-2}$.

The mismatch is readily explained by the fact that the electric field at the nozzle exit is higher than the nominal electric field.¹⁸

Although the drop generation process depicted in Fig. 1(b) appears steady, the cone-jet configuration has an intrinsic pulsation. The apparent steadiness results from a long integration time (0.4 ms); when the exposure time is reduced to 0.1 ms or less, intrinsic pulsations in the kilohertz range are observed. Marginean *et al.* provide insight into a similar intrinsic pulsation captured at $\sim 100\,000$ frames per second (fps).¹¹

In a drag-limited system, the flow rate that the EHD cone jet can accommodate is larger than the rate at which liquid can pass through the slender nozzle; this imbalance between loss and supply rates leads to intrinsic pulsations. Juraschek and Rollgen reported both low-frequency ($\sim 10 \text{ Hz}$) and high-frequency ($\sim 1 \text{ kHz}$) pulsation modes for an EHD configuration with a constant, externally pumped flow.¹⁰ The low-frequency mode is related to the depletion and filling of the cone and is not observed in our system where the flow rate is self-regulated (Sec. A3 of Ref. 13). Instead, the cone volume remains approximately constant after the cone is initially filled [as shown in Fig. 1(b)], and the intrinsic pulsations correspond to a high-frequency mode due to the mass ejection at the cone apex.

Building upon the work of Fernandez de la Mora⁸ and Fernandez de la Mora and Loscertales,¹² the scaling laws of the intrinsically pulsating cone jets in our system can be derived. For a “high-conductivity” liquid ($\geq 10^{-5} \text{ S/m}$) the intrinsically pulsating cone-jet transition is quasisteady, i.e., its lifetime is long compared to the time scale of charge redistribution which is on the order of the charge relaxation time.⁸ In the high-conductivity limit, the scaling laws of steady cone jet apply to the pulsating cone jets, including those for the flow rate, jet diameter, and convection current,¹²

$$Q_m \sim \gamma \tau_e \rho, \quad (3)$$

$$d_m \sim (\gamma \tau_e^2 / \rho)^{1/3}, \quad (4)$$

$$I_m \sim g(\epsilon) (\epsilon_0 \gamma^2 / \rho)^{1/2}, \quad (5)$$

where the subscript m denotes a scaling variable, ρ is liquid density, $g(\epsilon)$ is a factor accounting for the effects of dielectric constant of the liquid, which is experimentally measured,¹² and τ_e is the charge relaxation time defined as $\tau_e = \epsilon \epsilon_0 / K$, where ϵ and K are the dielectric constant and conductivity of the working liquid and ϵ_0 is the permittivity of vacuum. These scaling laws are expected to be valid for relatively conductive liquids when the jet diameter is much smaller than the characteristic nozzle dimension.¹⁹ In particular, Fernandez de la Mora and Loscertales experimentally showed that these scaling laws hold for water with various concentrations of ionic dopant and determined $g(\epsilon) \approx 18$ for aqueous solutions.¹²

The lifetime of the pulsating cone jets, i.e., the duration of a continuous jet within a pulsation cycle, can be derived by noting the analogous physics between pulsating cone jets on an isolated charged drop and those on a supported meniscus. The cone-jet transition develops when the surface charge accumulates to a level where the charge has to be redistributed to a larger surface area. The rate at which surface charge

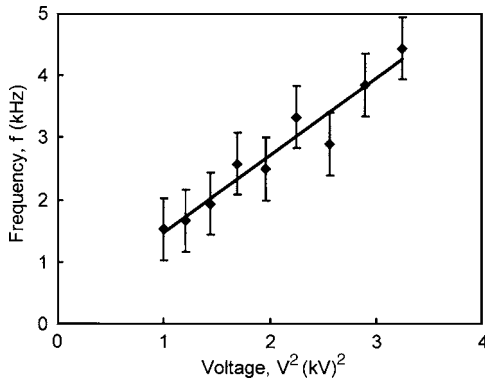


FIG. 3. Intrinsic pulsation frequency as a function of the applied voltage. For a system with $d=50\ \mu\text{m}$, $L=30\ \text{mm}$, and $S=110\ \mu\text{m}$, the intrinsic pulsation frequency was measured with a 10 000 fps camera using a $94\ \mu\text{s}$ exposure time. The error bars represent the maximum standard deviation of three independent measurements in the reported voltage range.

is accumulated and ejected determines whether the cone jet is transient or steady. For a pulsating cone jet, its lifetime is derived by integrating $dt=-dq/I$,⁸

$$\Delta t_{j,m} \sim \frac{\Delta q}{I_m} \sim \frac{\Delta q q_M}{q_M I_m} \sim \frac{\Delta q q_R}{q_R I_m} \sim C_{eq} \left(\frac{d_n}{d_m} \right)^{3/2} \tau_e, \quad (6)$$

where $\Delta t_{j,m}$ is the time scale for a drop with surface charge approaching the electrostatic stability limit (q_M) to release enough charge (Δq) before reaching a new electrostatic equilibrium and $C_{eq} \sim 1/g(\epsilon)\Delta q/q_R$ is a prefactor accounting for the dielectric effects and the charge loss ratio ($\Delta q/q_R$).⁸ Since only the convection current contributes to charge redistribution, I_m is used as the scaling for current in deriving the time scale for transient cone jets. Two assumptions are behind Eq. (6): (i) $q_M \sim q_R \sim \sqrt{\gamma\epsilon_0 d^3}$, where q_R is the Rayleigh limit for an isolated charged drop of diameter d ,²⁰ and (ii) $\Delta q/q_R$ is approximately constant (as in the case of a charged drop⁸).

The validity of jet lifetime scaling, Eq. (6), and its associated assumptions are supported by frequency measurement of the intrinsic pulsations. Based on the aforementioned scaling laws, one pulsation cycle extracts, from the cone, a volume of liquid,

$$V_{pj} \sim Q_m \Delta t_{j,m} \sim (d_n d_m)^{3/2}, \quad (7)$$

and the intrinsic pulsation frequency scales as

$$f_{pj} \sim \frac{Q}{V_{pj}} \sim \frac{Q_c}{(d_n d_m)^{3/2}} \sim \frac{KE^2}{\epsilon \mu L} \left(\frac{\rho d_n^5}{\gamma} \right)^{1/2}. \quad (8)$$

The validation of the scaling law, Eq. (8), for intrinsic pulsations is shown in Fig. 3. The pulsation frequency was measured by video imaging at 10 000 fps and spot-checked by the oscilloscopic current measurement detailed in Sec. A3 of Ref. 13. As the applied voltage is ramped up from 0 to 2 kV, the cone-jet transition sets in around 0.8 kV and the pulsation frequency increases from below 1 kHz at 0.8 kV to above 5 kHz at 2 kV. Between 1.0 and 1.8 kV, where non-linear, reproducible data were obtained, the pulsation frequency varied linearly with the voltage squared, which is consistent with the scaling law, Eq. (8).

The scaling law for intrinsic pulsations is further supported by the information shown in Fig. 1(b). The measured jet diameter (d_m) is $4 \pm 2\ \mu\text{m}$ and the inner diameter of the nozzle (d_n) is $50\ \mu\text{m}$. The scaling law, Eq. (7), indicates that the pulsating drop diameter, $(d_n d_m)^{1/2}$, should be $14 \pm 4\ \mu\text{m}$, which is consistent with the smallest drop diameter, $\sim 10\ \mu\text{m}$, measured at 3.6 ms.

The scaling laws for intrinsic pulsation provide important design guidelines for EHD drop formation as demonstrated by Chen *et al.*²¹ The jet diameter scaling, Eq. (4), is a lower bound to the positioning accuracy of the drop. The volume per pulsation, Eq. (7), determines the smallest EHD drop. The pulsation frequency, Eq. (8), is an upper bound for the speed of drop generation. The scaling laws of EHD flow rates and cone-jet pulsations are also expected to be applicable to miniaturized electro spraying provided that the assumptions such as thin nozzle and high conductivity are properly satisfied.

This work was supported by Directed Technologies Inc., NASA Biologically Inspired Materials Institute (BIMat) under Award No. NCC-1-02037, and ARO-MURI under Award No. W911NF-04-1-0170. The authors thank S. Korkut for helpful discussions and D. M. Dabbs in the preparation of the letter.

¹O. A. Basaran, *AIChE J.* **48**, 1842 (2002).

²A. U. Chen and O. A. Basaran, *Phys. Fluids* **14**, L1 (2002).

³O. Yogi, T. Kawakami, M. Yamauchi, J. Y. Ye, and M. Ishikawa, *Anal. Chem.* **73**, 1896 (2001).

⁴M. Cloupeau and B. Prunet-Foch, *J. Aerosol Sci.* **25**, 1021 (1994).

⁵P. M. Adornato and R. A. Brown, *Proc. R. Soc. London, Ser. A* **389**, 101 (1983).

⁶O. A. Basaran and L. E. Scriven, *Phys. Fluids A* **1**, 795 (1989).

⁷O. A. Basaran and L. E. Scriven, *Phys. Fluids A* **1**, 799 (1989).

⁸J. Fernandez de la Mora, *J. Colloid Interface Sci.* **178**, 209 (1996).

⁹J. F. Wei, W. Q. Shui, F. Zhou, Y. Lu, K. K. Chen, G. B. Xu, and P. Y. Yang, *Mass Spectrom. Rev.* **21**, 148 (2002).

¹⁰R. Juraschek and F. W. Rollgen, *Int. J. Mass. Spectrom.* **177**, 1 (1998).

¹¹I. Marginean, L. Parvin, L. Heffernan, and A. Vertes, *Anal. Chem.* **76**, 4202 (2004).

¹²J. Fernandez de la Mora and I. G. Loscertales, *J. Fluid Mech.* **260**, 155 (1994).

¹³See EPAPS Document No. E-APPLAB-89-001638: Sec. A1, details of experimental setup; Sec. A2, empirical equivalence of cone and drop formation rates; and Sec. A3, pulsation frequency measured by EHD current. The document may also be reached via the EPAPS homepage (<http://www.aip.org/pubservs/epaps.html>) or from <ftp.aip.org> in the directory /epaps/. See the EPAPS homepage for more information.

¹⁴M. S. Wilm and M. Mann, *Int. J. Mass Spectrom. Ion Process.* **136**, 167 (1994).

¹⁵T. D. Wood, M. A. Moy, A. R. Dolan, P. M. Bigwarfe, T. P. White, D. R. Smith, and D. J. Higbee, *Appl. Spectrosc. Rev.* **38**, 187 (2003).

¹⁶N. B. Cech and C. G. Enke, *Mass Spectrom. Rev.* **20**, 362 (2001).

¹⁷G. I. Taylor, *Proc. R. Soc. London, Ser. A* **280**, 383 (1964).

¹⁸M. T. Harris and O. A. Basaran, *J. Colloid Interface Sci.* **161**, 389 (1993).

¹⁹As pointed out by Fernandez de la Mora (Ref. 8) and Fernandez de la Mora and Loscertales (Ref. 12) the flow rate scaling [Eq. (3)] is the minimum attainable, which is the correct scaling for pulsating cone-jet transition. Phenomenologically, pulsation takes place when the supply rate of liquid to the cone is less than the loss rate through the cone jet (Ref. 10). It is unlikely for a self-regulating system to select a higher flow rate than necessary (i.e., the minimum), as a higher flow rate leads to more rapid and severer imbalance of mass flow.

²⁰Lord Rayleigh, *Philos. Mag.* **14**, 184 (1882).

²¹C.-H. Chen, D. A. Saville, and I. A. Aksay, *Appl. Phys. Lett.* **88**, 154104 (2006).